Coherent RF Error Statistics

ROBERT B. DYBDAL, MEMBER, IEEE, AND RANDOLPH H. OTT, SENIOR MEMBER, IEEE

Abstract —RF error statistics for power, voltage, and phase are derived under the assumptions that the error component is coherently related to the desired signal, that its magnitude is constant, and that its phase is equally likely and uniformly distributed from 0 to 360°. The error statistics which result from these assumptions have nonzero mean values for power and voltage and standard deviations which differ significantly from those projected on the basis of Gaussian statistics that apply to incoherent errors. These statistics will be applied to typical component errors which arise in an overall system error budget.

I. INTRODUCTION

THE ACCURACY of RF measurements is a fundamental assessment in experiment design, measurement programs, and system evaluations. Projections of overall measurement accuracy are typically made through error budget assessments comprised of an rss sum of the random error components added to the sum of bias error components. The error budget, therefore, requires knowledge of the individual error mechanisms and quantification of their first- and second-order statistics, i.e., the mean and rms error values. Over the years, Gaussian statistics have been widely used in error projections dating to the original application by Woodward [1]. A tutorial presentation of this analysis, its underlying validity, and applications was presented by Swerling [2], and the extent of such applications is described in [3]. Further extensions of this analysis continue into the present time; the statistics for the phase difference between two vectors have recently been published [4]. These analyses, however, are tied to the fundamental assumption of Gaussian statistics.

When errors are coherently related to the desired signal, the assumption of additive Gaussian error statistics conflicts with physical interpretation. The error statistics for the coherent case are derived on the basis of the familiar phasor diagram shown in Fig. 1, where the true value is set to unity with a 0° phase angle without loss of generality, and the error has a constant relative amplitude a and phase angle α, which is assumed to be equally likely and uniformly distributed from 0 to 360°. The physical model of this situation is particularly appropriate with today's popularity for swept-frequency measurements. Generally, the magnitude of the error component varies slowly with frequency changes while the phase between the true and error components rotates with frequency changes. This

phasor picture of the errors has had most application and familiarity in terms of the peak-to-peak values of the error. However, the first- and second-order statistics for this distribution have had relatively little investigation and are believed to be original in this work. The simple phasor diagram is adequate for narrow-bandwidth signals; for broader bandwidth waveforms, the error component should be weighted by the autocorrelation of the waveform with the appropriate time delay.

If both the amplitude and phase of the error component can be determined, then the error can, of course, be quantified deterministically by calibration. Indeed, this technique is well developed in modern network analyzer practice, where vector measurement techniques used with reference standards obtain the full scattering matrix characterization of the measurement system [5]. In this case, measurement accuracy is exceedingly good, and is limited principally by the repeatability of the setup, accuracy of the standards, quantization in the sampling, etc. However, the coherent errors cannot always be determined through calibration, and in some situations, e.g., multipath, the phasing of the error component may be time-varying. These statistics are also useful in specifying the component performance needed to achieve overall system performance.

II. STATISTICAL ANALYSIS

This section develops the necessary analyses for the first- and second-order statistics for power, voltage, and phase measurements. The resulting statistics will be compared to the more familiar Gaussian error statistics.

A. Statistics for Power

The error statistics for power measurements are straightforward to derive. With reference to Fig. 1, the total power measured is given by

$$P = (1 + ae^{j\alpha})(1 + ae^{j\alpha})^*$$
$$= 1 + a^2 + 2a\cos\alpha. \tag{1}$$

The mean value of the resultant power is obtained from

$$E_P = (1/2\pi)\int_0^{2\pi}(1 + a^2 + 2a\cos\alpha)\,d\alpha$$
$$= 1 + a^2. \tag{2}$$

The true power level, which would be observed when a equals zero, is unity, so that the mean power error equals a^2. Similarly, the variance of the resultant power is ob-
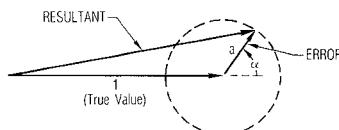
Fig. 1.   Phasor diagram for coherent error analysis.
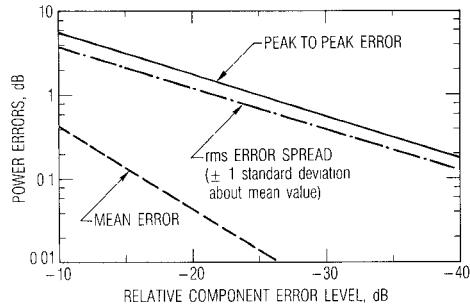
Fig. 2.   Power error statistics.

TABLE I
COMPUTATION COMPARISON FOR MEAN VALUE
OF THE TOTAL VOLTAGE

a	IMSL Subroutine Integration	Eq. (6) $(1+a)(1-\dfrac{a}{(1+a)^2})$	Eq. (7) $1 + (a^2)/4$
.000	1.00000000	1.00000000	1.00000000
.100	1.00250157	1.00909091	1.00250000
.200	1.01002525	1.03333333	1.01000000
.300	1.02262952	1.06923077	1.02250000
.400	1.04041709	1.11428571	1.04000000
.500	1.06354441	1.16666667	1.06250000
.600	1.09223858	1.22500000	1.09000000
.700	1.12682867	1.28823529	1.12250000
.800	1.16780951	1.35555556	1.16000000
.900	1.21600092	1.42631579	1.20250000
1.000	1.27323928	1.50000000	1.25000000

tained from

$$V_P = (1/2\pi)\int_0^{2\pi}(P - E_P)^2\, d\alpha$$

$$= 2a^2 \tag{3}$$

and the corresponding standard deviation is given by

$$\sigma_P = \sqrt{2}\, a. \tag{4}$$

Typical values for the error statistics are plotted in Fig. 2 in the form of dB values. The peak-to-peak levels, which are commonly seen as the modulation envelope of coherent interaction, are presented. The mean error has an appreciable value as a increases. Because of the logarithmic form of the dB values, $a \pm 1\sigma$ spread about the mean value of the power is presented in this figure.

B. Statistics for Voltage

The statistics for voltage errors are not as simply derived as the power errors. The total voltage is the square root of (1), and the error is obtained by subtracting unity, the true value. The mean value of the total voltage is

$$E_V = (1/2\pi)\int_0^{2\pi}V\, d\alpha$$

$$= (2/\pi)(1 + a)E\big(4a/(1 + a)^2\big) \tag{5}$$

where $E(\ )$ is the complete elliptic integral of the second kind. While the elliptical integral is tabulated, a simple analytic expression is more useful. Two polynomial approximations for the elliptic integral [6] were examined; the polynomial series were derived for the argument and the complement of the argument. The series based on the argument results in

$$E_V \approx (1 + a)\Big(1 - \big(a/(1 + a)^2\big) - \big(3a^2/4(1 + a)^4\big)\cdots\Big). \tag{6}$$

The series based on the complementary argument results in

$$E_V \approx 1 + (a^2/4) + (a^4/64) + \cdots. \tag{7}$$

Numerical comparisons of the expressions derived for the expected value of the total voltage were made. The elliptic integral was computed from an IMSL subroutine based on Chebyshev polynomials available on our computer system, numerical integration of the integral using a trapezoidal rule with 1000 points, and the two series expansions given in (6) and (7). The results of these comparisons are presented in Table I in terms of the expected value of the total voltage; the expected error is obtained by subtracting 1 from these numbers. The exact value for $a = 1$ can be derived analytically and is equal to $4/\pi$, which provides another check. The series presented in (7) provides not only the most accurate series result, but also the most convenient form to compute. For $a < 0.5(- 6$ dB), the accuracy of the mean error computed from $(1/4)a^2$ is within 1.6 percent.

The second-order statistics for the voltage were also derived. The expected value of the square of the voltage is identical with the expected value of the power given in (2). The variance of the total voltage is given by

$$V_V = 1 + a^2 - \big((2(1 + a)/\pi)E\big(4a/(1 + a)^2\big)\big)^2. \tag{8}$$

The computation of the elliptic integral arises again. The first two terms of (7) result in the following expression for the standard deviation:

$$\sigma_V \approx (a/\sqrt{2})\big(1 - (3a^2/16) - \cdots\big)^{1/2}. \tag{9}$$

The results of a numerical comparison between this expression and (8) evaluated by the Chebyshev polynomial routine are presented in Table II. For $a < 0.5$ ($- 6$ dB), the expression in (9) is accurate within 0.1 percent. Values of the peak-to-peak variations, the mean error, and the rms spread about the mean for the voltage are plotted in Fig. 3.

C. Statistics of Phase

The statistics for the phase are difficult to derive in closed form. Again, referring to the phasor diagram in Fig.

TABLE II
COMPUTATION COMPARISON FOR STANDARD DEVIATION OF
VOLTAGE ERRORS

a	IMSL Subroutine	Eq. (9)
.000	.00000000	.00000000
.100	.07064423	.07064436
.200	.14088642	.14089003
.300	.21030662	.21033456
.400	.27844620	.27856777
.500	.34478005	.34516753
.600	.40867453	.40969501
.700	.46931562	.47168912
.800	.52556726	.53065997
.900	.57562294	.58608073
1.000	.61551690	.63737744

TABLE III
COMPUTATIONAL COMPARISON FOR STANDARD DEVIATION OF
PHASE ERRORS

| a	Numerical Integration*	Eq. (12)
0	0	0
0.1	4.08	4.06
0.2	8.24	8.14
0.3	12.31	12.29
0.4	16.59	16.53
0.5	20.98	20.88
0.6	25.92	25.38
0.7	30.12	30.05
0.8	35.92	34.91
0.9	42.54	39.98
1.0	51.96	45.30

*Values in degrees.
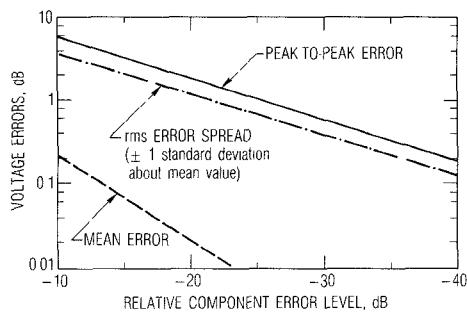
Fig. 3. Voltage error statistics.
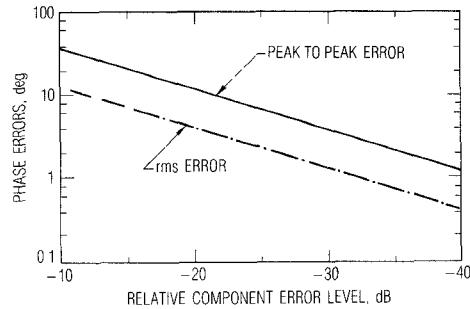
Fig. 4. Phase error statistics.

1, the error in the phase can be expressed as

$$\epsilon = \tan^{-1}(a\sin\alpha/(1 + a\cos\alpha)). \qquad (10)$$

The mean value of the phase error can be analytically demonstrated to be zero by observing the symmetry of the integrand used to calculate the expected value. The second-order statistics can be derived from

$$V_\phi = (1/2\pi)\int_0^{2\pi}(\epsilon)^2\,d\alpha. \qquad (11)$$

This integral is difficult to evaluate in closed form. If the integrand is expanded in a Taylor's series, the following expression results:

$$V_\phi \approx a^2/2 + a^4/8 + \cdots \qquad (12)$$

and the standard deviation is obtained from the square root of these values. Table III shows a comparison of the series approximation with the numerical evaluation of the integral for the standard deviation values. For $a < 0.5$ (-6 dB), the accuracy of the series form compared to the numerical integration is better than 0.5 percent. The case $a = 1$ can also be integrated exactly, with the result $\pi^2/12$, which provides another check on the results.

Values for the peak-to-peak errors and the standard deviation for the phase are also presented in Fig. 4. The peak-to-peak errors are the modulation envelope of the phase ripple observed experimentally.

D. Summary and Comparison

For convenience, the expressions for the mean and standard deviation of the errors are presented in Table IV. The approximate expressions derived from series expansions are indicated by $\approx$. These statistics are for the error values; the correct value of 1 has been taken out.

The comparison between the statistical values derived for the coherent errors and those derived from the Gaussian statistics was done in the following manner. The standard deviation for Gaussian statistics is typically derived by assuming that the peak-to-peak variations represent $\pm 5\sigma$ values, with the results for power, voltage, and phase given in Table IV. The standard deviations for the coherent error case are significantly higher than those for the incoherent case. In addition, the coherent error statistics for both power and voltage have nonzero mean errors, in contrast to the incoherent case.

The theoretical basis of the coherent and incoherent error statistics also provides a contrast between the two types of error components. The statistics for incoherent errors are derived under the assumption of a large number of statistically similar components having a zero mean error. The central limit theorem is then invoked to obtain Gaussian statistics [7]. As will be discussed, many practical microwave measurement applications do not have a "large" number of statistically similar components. The question

TABLE IV
COMPARISON OF ERROR STATISTICS

	Mean	rms
Coherent		
Power	a^2	$\sqrt{2}\,a$
Voltage	$\approx a^2/4$	$\approx a/\sqrt{2}$
Phase	0	$\approx a/\sqrt{2}$
Incoherent ($\pm\,5\sigma$)		
Power	0	0.4 a
Voltage	0	≈ 0.2 a
Phase	0	≈ 0.2 a

of "largeness" has been explored further [8], [9]. These analyses can be applied in the case of the statistics for voltage, and are based on the random walk problem. The random walk problem is typically approached in a series of steps, with the overall distance, which corresponds to voltage in this context, expressed by Kluyver's formula [10]. Kluyver's formula gives the probability of the resultant distance as a product of Bessel functions whose arguments depend on the individual step size. In the problem depicted in Fig. 1, two steps, 1 and a, are taken. It can be shown that the same series given in (7) is obtained from the random walk treatment of the problem.

III. APPLICATIONS

Typical applications for the statistical analyses which have been developed are described here. This discussion concentrates on those measurement applications in which the full vector characterization and calibration of the measurement system as used in modern network analyzer systems are not practical; such examples are seen in RF measurements performed in open systems, and three such applications are described. The manner in which the receiver processes information also dictates the appropriate application of the statistics of power, voltage, or phase.

A. RF Facility Limitations

Antenna and RCS (radar cross section) measurements are performed in open facilities whose inherent background returns limit measurement accuracy. These facilities, whether outdoor ranges or indoor anechoic chambers, strive to provide a free-space environment for the antenna or radar target under test, and the measurement errors for the facility result from the deviation from an ideal free-space environment. The facility is illuminated by the same signal used to evaluate the antenna or radar target; consequently, the errors are coherently related to the desired signal.

Reflectivity is the measure of the facility background for antenna measurements. The physical basis of this term is the ratio of the reflected energy from the facility to the energy in the desired direct signal. The mechanisms of reflectivity may be either distributed, as in the walls of an anechoic chamber, or discrete, as in reflecting objects in outdoor ranges. The application of this term is illustrated by the pattern measurement depicted in Fig. 5(a). Reflec-
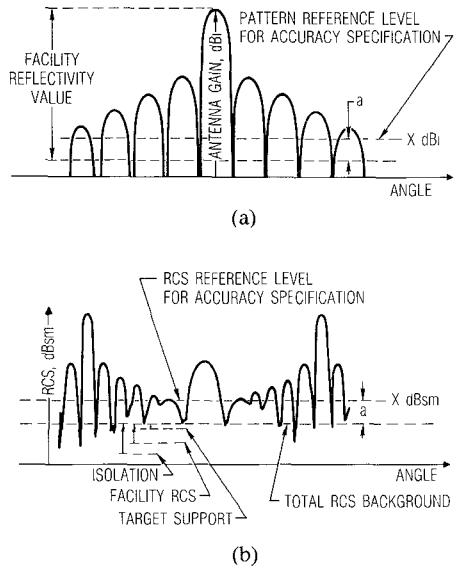

Fig. 5.   RF facility measurement errors. (a) Antenna pattern measurements. (b) Radar cross section measurements.

tivity is referenced to the peak gain level of the measured antenna pattern. When the reflectivity equals the dynamic range of the pattern measurement, the facility reflects as much power as that received by the true antenna pattern measured in an ideal free-space environment. Generally, antenna pattern accuracy is specified at an absolute gain level, and the difference between that level and the reflectivity level of the facility determines the value of a as used here. In the illustration, the reflectivity level is indicated as a constant level; when discrete reflection sources exist in a facility, the reflectivity varies with aspect angle.

The RCS facility background is somewhat more complex. Three mechanisms contribute to the background level of the facility: 1) the radar return from the physical structure of the facility, 2) the radar return from the target support system, and 3) the finite isolation between the instrumentation radar's transmitter and receiver. These three mechanisms are treated independently in error budgets, and are referenced to an absolute RCS level at the range at which the target is measured. RCS measurement accuracy is generally specified at an absolute RCS level, and the value of a is determined for each mechanism relative to that specified level, as depicted in Fig. 5(b). The aggregate error for the three independent mechanisms can be obtained from an rss sum added to the sum of the mean values. This process can be easily justified by generalizing the power statistics to N phasors appropriate to the definition of RCS. Therefore, this combination of the three mechanisms to form an aggregate background level of the RCS facility is valid.

Both antenna gain and RCS are defined on the basis of power, and the power error statistics previously derived can be directly applied. Voltage and phase statistics have more limited application for RF facility limitations. One example lies with RCS measurements in which the polarization properties of radar targets are to be transformed from one orthogonal set to another, i.e., from linear to

circular. In this case, amplitude and relative phase measurements are required, and the scattering matrix treatment developed by Kennaugh [11] is used. The statistics for voltage and phase can be applied to assess measurement accuracy in this case.

B. Multipath

Statistical analyses have been widely used to project the performance of RF systems that operate in a multipath environment. A statistical treatment for multipath is particularly appropriate because in many applications the phasing between the multipath components is time-varying. The time variation can result from changes in the link geometry, changes in refraction characteristics, or, in the case of ionospheric propagation, changes in the plasma profiles. The statistical treatments for such problems have used Rayleigh or Rician distributions [12]. These statistical treatments provide an interesting contrast to the coherent error analyses presented here.

The distinction between the coherent error analyses and Rayleigh or Rician statistics lies with the number of components. As formulated here, the statistics consider the case in which two components comprise the total field. By contrast, Rayleigh statistics assume an infinite number of components with the same statistical distribution, while the Rician statistics assume one dominant component together with a Rayleigh-distributed infinite number of components [12]. Indeed, both distributions can be derived by expanding the number of terms in Kluyver's formula, used in the random walk problem. More general distributions are treated in [13]. In contrast with these statistical assumptions, many practical microwave problems have only a limited number of error components. The treatment of a limited number of components has received less attention [8], [9]. The numerical results suggest that at least five or six components are required for the probability to approach the Rayleigh distribution.

The statistical analyses for the coherent errors treat a direct signal, represented by unit amplitude, and one multipath component, represented by the relative amplitude a. The statistical analyses therefore apply to the classic geometric optics picture of propagation over a smooth, flat ground. The Fresnel reflection coefficients [14] adjusted by any differential space loss and antenna pattern factor can be used to estimate the value of a for a given polarization. Again, the appropriate statistical value can be selected according to the manner in which the receiver processes the RF signal.

C. Antenna Cross-Polarization Errors

The cross-polarization inherent in practical antenna designs leads to other applications for the statistical analyses developed here. The cross-polarization errors for a single antenna are one example. The measurement of the power and polarization characteristics of an incident field by two nominally orthogonally polarized antennas is a second example. Polarization concepts are described in more detail in [15].

Pattern measurements of antennas typically characterize the relative amplitudes of the principal and cross-polarized components. Measurements of the relative phase between principal and cross-polarized components can be performed, albeit with additional measurement expense and calibration uncertainty. The analysis presented here can be used by equating the relative level of the cross-polarized response to the parameter a used in the statistical analysis. The choice of power, voltage, and/or phase statistics again depends on the manner in which the receiver processes the information.

The second application related to cross-polarization for this statistical analysis lies with those systems designed to measure the polarization of incident fields. Ideally, the characterization is performed with two orthogonally polarized antennas; in practice, some level of cross-polarization exists and the two antennas are only nominally orthogonally polarized. In some cases, the voltages received by these two antennas with their inherent cross-polarization can be expressed as

$$\begin{bmatrix} V_1 \\ V_2 \end{bmatrix} = \begin{bmatrix} 1 & \Gamma \\ \Gamma & 1 \end{bmatrix} \begin{bmatrix} b \\ \sqrt{1-b^2}\big/\beta \end{bmatrix} \qquad (13)$$

where V_1 and V_2 are the voltages at the nominally orthogonal output ports of the antenna, Γ is the complex value of the antenna cross-polarization, and b and $\sqrt{1-b^2}\big/\beta$ are the incident field components resolved into orthogonal components. The incident field is specified in this fashion to express the most general elliptically polarized incident field on the two antennas. A simple example of such a system which obeys (13) is two orthogonal dipoles connected through a hybrid network.

If the two antennas were ideally orthogonally polarized, the total power in the incident field could be obtained by simply summing the power in each antenna port. The power received by the two ports is given by

$$P_p = 1 + \Gamma^2 + 4b\sqrt{1-b^2}\cos\beta\,\mathrm{Re}\,\Gamma. \qquad (14)$$

It can be shown that the worst-case errors in the power measurement occur when $b = 1/\sqrt{2}$ and $\cos\beta = \pm 1$. Under these conditions, this power expression reduces to (1). Physically, these two conditions correspond to ideally linear or circularly polarized incident fields transmitted with either the same or opposite phasing. It is interesting to note that these are the most common choices of orthogonally polarized fields.

The measurement of an incident field which is ideally linearly polarized is another typical task. The polarization characteristics of the antenna, the parameters 1 and Γ is (13), are commonly specified in either orthogonal linear or orthogonal circular components. The incident power and orientation of the electric field, the latter referred to as tilt angle, are typically the quantities to be determined by such systems. The errors in such a measurement are described in Table V. The orientation, or tilt angle, of the field is expressed by θ, which is defined 0 to 180°. The functional form of the errors in Table V therefore reduces to the same

TABLE V
CROSS-POLARIZATION ERRORS FOR LINEARLY POLARIZED FIELD

	Measured by Linearly Polarized Antenna	Measured by Circularly Polarized Antenna
b	$\cos\theta$	$1/\sqrt{2}$
$\sqrt{1-b^2}\ \underline{/\beta}$	$\sin\theta$	$(1/\sqrt{2})\ \underline{/2\theta}$
Power Error	$\Gamma^2 + 2\sin2\theta\ \mathrm{Re}\,\Gamma$	$\Gamma^2 + 2\cos2\theta\mathrm{Re}\,\Gamma$
Mean Power Error	Γ^2	Γ^2
rms Power Error	$\sqrt{2}\ \mathrm{Re}\,\Gamma$	$\sqrt{2}\ \mathrm{Re}\,\Gamma$
Tilt Angle	$\tan^{-1}|v_2/v_1|$	$1/2\ \Delta\phi$
Indicated Tilt Angle	$\tan^{-1}\left(\frac{\sin\theta\,+\,\Gamma\cos\theta}{\cos\theta\,+\,\Gamma\sin\theta}\right)$	$\tan^{-1}\left(\tan\theta\,(\frac{1-\Gamma}{1+\Gamma})\right)$
Error in Tilt Angle	$\tan^{-1}\left(\frac{\Gamma\cos2\theta}{1\,+\,\Gamma\sin2\theta}\right)$	$\tan^{-1}\left(\frac{\Gamma\sin2\theta}{1\,+\,\Gamma\cos2\theta}\right)$
Mean Tilt Angle Error	0	0
rms Tilt Angle Error	$\approx \Gamma/\sqrt{2}$	$\approx \Gamma/\sqrt{2}$

Fig. 6. VSWR interaction. (a) Block diagram. (b) First-order interaction.

form as those used in the statistical analysis previously described. The power errors are identical to those previously discussed, and the tilt angle errors correspond to those for the phase error analysis, and the analyses presented here also apply. The errors for more generally polarized incident fields are described in [16].

D. VSWR Interaction

The VSWR interaction between connecting electronic components is the final application discussed here. Modern network analyzer systems use vector calibration to minimize such errors; however, such instrumentation is not always available. The statistical approach also finds application when component requirements must be specified in an error budget projecting overall operational system performance.

A first-order VSWR interaction is shown in Fig. 6. Reference planes associated with the two electronic components are indicated by the subscripts, and the two components are assumed to be connected by a cable of length d and phase velocity k. The ratio of the direct transmission to the first interaction as derived in this figure is given by

$$R = \Gamma_1\Gamma_2 e^{-j2kd}$$
$$= |R|\underline{/\rho}\ .\qquad(15)$$

This derivation provides both amplitude and phase information so that the interaction effects can be arrived at deterministically. In many cases, however, only VSWR data are available as a description of the terminals, and the phase information is lost. In such cases, the statistical description developed here is appropriate. The value of a expressed in terms of the scalar VSWR parameter is given by

$$|R| = \frac{\mathrm{VSWR}_1 - 1}{\mathrm{VSWR}_1 + 1}\frac{\mathrm{VSWR}_2 - 1}{\mathrm{VSWR}_2 + 1}\qquad(16)$$

where the subscripts on the VSWR quantities are associ-

ated with the two terminal planes. The parameter $|R|$ can be equated to a and the statistical analyses can be applied.

The analysis thus far has considered only the first-order interactions; the higher order interactions become significant only when both VSWR values are large. The effects of these higher order interactions are conventionally written in closed form by observing that each succeeding interaction equals the preceding interaction multiplied by R. The total VSWR interaction is thus expressed by

$$R' = R/(1 - R)$$
$$= |R'|\underline{/\rho'}\ .\qquad(17)$$

This expression can also be inverted to yield

$$R = R'/(1 + R').\qquad(18)$$

Examining the phase of these expressions yields

$$\rho = \rho' - \rho''$$

where

$$\rho'' = \tan^{-1}(|R|\sin\rho/(1 - |R|\cos\rho)$$
$$= \tan^{-1}(|R'|\sin\rho'/(1 + |R'|\cos\rho').\qquad(19)$$

Thus, the statistics of the phase of the higher order interactions have the same functional form as the phase statistics previously derived.

The effect of the magnitude of the higher order interaction terms can be treated statistically. The magnitude of R' is given by

$$|R'| = |R|/(1 + |R|^2 - 2|R|\cos\rho)^{1/2}.\qquad(20)$$

The highest level reflection value is given by

$$|R'|_{\max} = |R|/(1 - |R|)$$
$$= (\mathrm{VSWR}_1 - 1)(\mathrm{VSWR}_2 - 1)$$
$$/(2(\mathrm{VSWR}_1 + \mathrm{VSWR}_2)).\qquad(21)$$

This represents the worst-case VSWR interaction and is plotted in Fig. 7 for representative VSWR values. The
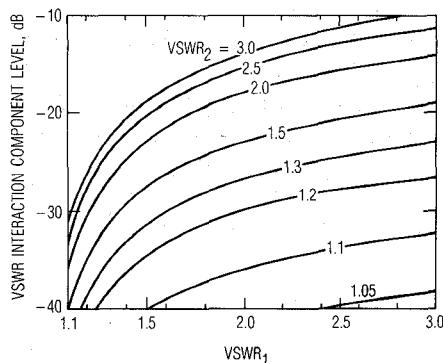
Fig. 7. Worst-case VSWR interaction errors.
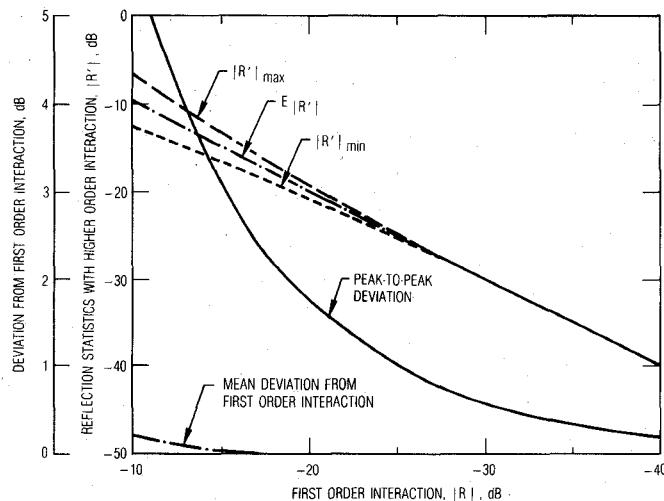
Fig. 8. Statistics for total VSWR interaction magnitude relative to first-order interaction values.

minimum level reflection value is given by

$$|R'|_{\min} = |R|/(1+|R|). \qquad (22)$$

The mean value of the VSWR interaction can be calculated by assuming ρ to be uniformly distributed from 0 to 360°. The result is

$$E_{|R'|} = \left(2|R|/\pi(1+|R|)\right) K\left(2\sqrt{|R|}/(1+|R|)\right) \qquad (23)$$

where $K(\ )$ is the complete elliptic integral of the first kind. Series expressions for the elliptic integral were examined [6], and a form based on the complementary argument was found both accurate and computationally convenient; the expression is

$$E_{|R'|} \approx |R|\left(1+\left(|R|^2/4\right)+\left(9|R|^4/64\right)+\cdots\right. \qquad (24)$$

The accuracy of this expression is better than 1.0 percent for $a < 0.5$ (-6 dB), and also provides a convenient means to assess the effects of higher order interactions in an average sense. Numerical values for the effects of the higher order interaction statistics are presented in Fig. 8.

IV. SUMMARY

The statistics for coherent power, voltage, and phase errors are derived under the assumptions that the amplitude of an error component has a constant level and that

the phase of the component is unknown and equally likely and uniformly distributed between 0 and 360°. These statistics differ from the values projected from Gaussian statistics which apply to incoherent errors. In many practical microwave measurements, the number of statistically similar components is not large, and the coherent errors are better characterized by this statistical model. Several applications are cited in which the vector calibration necessary to determine the phase angle α is impractical.

ACKNOWLEDGMENT

REFERENCES

[1] P. M. Woodward, Probability and Information Theory with Applications to Radar. New York: McGraw-Hill, 1953.

[2] P. Swerling, "Parameter estimation accuracy formulas," IEEE Trans. Inform. Theory, vol. IT-10, pp. 302-314, Oct. 1964.

[3] D. K. Barton and H. R. Ward, Handbook of Radar Measurement. Englewood Cliffs, NJ: Prentice-Hall, 1969.

[4] R. F. Pawula, S. O. Rice, and J. H. Roberts, "Distribution of the phase angle between two vectors perturbed by Gaussian noise," IEEE Trans. Commun., vol. COM-30, pp. 1828-1841, Aug. 1982.

[5] _____, "Automating the HP 8410B Microwave Network Analyzer," Hewlett Packard Application Note 221A, June 1980.

[6] I. S. Gradshteyn and I. M. Ryzhik, Table of Integrals, Series, and Products. New York: Academic Press, 1965, pp. 904-906.

[7] D. Middleton, An Introduction to Statistical Communication Theory. New York: McGraw-Hill, 1960, chs. 7 and 9.

[8] W. R. Bennett, "Distribution of the sum of randomly phased components," Quart. Appl. Math., vol. 5, pp. 385-393, Jan. 1948.

[9] M. Slack, "Probability densities of sinusoidal oscillations combined in random phase," J. IEE, vol. 93, part III, pp. 76-86, 1946.

[10] G. N. Watson, A Treatise on the Theory of Bessel Functions. Cambridge, 1944, p. 420.

[11] E. M. Kennaugh, Research Studies on the Polarization Properties of Radar Targets (Commemorative Volume I and II, ElectroScience Laboratory). The Ohio State University, July 1984.

[12] P. Beckmann, Probability in Communication Engineering. New York: Harcourt, Brace, 1967, chs. 4 and 5.

[13] P. Beckmann and A. Spizzichino, The Scattering of Electromagnetic Waves from Rough Surfaces. Elmsford, NY: Pergamon, 1963, ch. 7.

[14] J. A. Stratton, Electromagnetic Theory. New York: McGraw-Hill, 1941, pp. 490-511.

[15] _____, IEEE Standard Test Procedures for Antennas, IEEE Standard 149, 1979, ch. 11.

[16] R. B. Dybdal, "Cross polarization errors in RF measurements," in Proc. Second Workshop on Polarimetric Radar Technology (Huntsville, AL), May 3-5, 1983.

✻
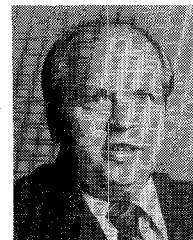
Robert B. Dybdal (S'63-M'70) was born in Dayton, OH, on August 2, 1941. He received the B.S.E.E. and M.Sc. degrees in 1964 and the Ph.D. degree in 1968 in electrical engineering from Ohio State University, Columbus.

From 1963 to 1968, he was employed as a Research Associate at the ElectroScience Laboratory, Ohio State University, where he was engaged in research on antennas, diffraction theory, transient radar scattering, and waveguides with impedance surfaces. In 1968, he joined the Aerospace Corporation and is presently the Manager of the RF Systems Research Office. His research interests include component and system development of communication, radar, and radiometric designs and RF measurement techniques.

Dr. Dybdal is a member of Eta Kappa Nu, Sigma Xi, and URSI Commission B.
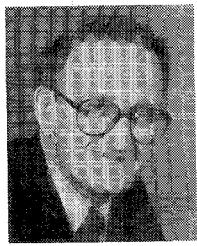
Randolph H. Ott (S'62–M'63–SM'76) was born in New Glarus, WI, on September 20, 1936. He received the B.S. degree from the University of Wisconsin, Madison, in 1959 and the M.S. and Ph.D. degrees from The Ohio State University, Columbus, in 1961 and 1966, respectively, all in electrical engineering.

In November 1966, he joined the U.S. Department of Commerce, Office of Telecommunications, Institute for Telecommunication Sciences, Boulder, CO. Dr. Ott joined the International Telecommunications Union–International Radio Consultative Committee (CCIR), Geneva, Switzerland, in 1980. From 1982 to 1983, he was a staff scientist at COMSAT Labs. in Clarksburg, MD. In 1983, Dr. Ott joined The Aerospace Corporation and works in the Space Technology Center in Albuquerque, NM.

Dr. Ott was an Associate Editor for IEEE TRANSACTIONS ON ANTENNAS AND PROPAGATION for the years 1979–1980. He has served as Chairman of the Denver–Boulder chapters of both the IEEE Society for Communications and the Antennas and Propagation Society. He is a member of Pi Mu Epsilon, Sigma Xi, Commissions B, C, and F of the International Union of Radio Science, and the Mathematical Association of America.